Rational design of inhibitors against TAR DNA-binding protein 43 (TDP-43) to prevent neurodegenerative disorders

ASWANTH SULOCHANAN NAIR[1,2] AND GAURAV SHARMA[2]

[1]Lambert High School, Suwanee, Georgia
[2]Eigen Sciences, NC, Apex

Published Dec, 2024

TAR DNA-binding protein (TDP-43) is primarily found in the nucleus and has a vital function in the processing of RNA/DNA and the control of genes. Mutations in this protein are linked to neurodegenerative diseases such as amyotrophic lateral sclerosis (ALS) and frontotemporal dementia (FTD) and inhibiting the mutated protein will help in preventing these diseases. Due to the complex and flexible nature of the protein the complete 3D structure of this protein is complicated to obtain. In our work, we have used computational strategies like structure elucidation techniques to profit the DNA-bound three-dimensional structure of this protein. In addition, molecular docking simulations were performed to identify inhibitors capable of binding to the mutated RRM1 protein, thus preventing the mutated protein functioning. Our hypothesis is that that docking ligands binds to the portions of the protein that bind to DNA and prevent the DNA binding to the mutate protein. According to our research, we have identified five chemical compounds that have a high affinity for RRM1 protein. All the ligands bind to the DNA interacting domain of the RRM1 protein. In addition, we have also predicted the complete three-dimensional configuration of DNA bound TDP-43 protein complex and according to our understanding, this is the first time the complex 3D structure has been reported. Based on the elucidated structure and electrostatic surface potential the negatively charged DNA binds only to the positively charged RRM1 domain of the TDP-43 protein. The current investigation will help in developing novel therapeutics against neurodegenerative diseases.

1. INTRODUCTION

A mutated TDP-43 is a cause for various neurodegenerative diseases, such as amyotrophic lateral sclerosis (ALS), and frontotemporal dementia (FTD) (1). TDP-43 interacts with various binding proteins in DNA/RNA processing before that strand is sent to be translated into a protein (2). TDP-43 is also responsible for some aspects of protein degradation (2). Additionally, TDP-43 has been seen to interact with transcription factors for gene expression and regulation (2). All of these are important aspects needed for a cell to function. If a mutation occurs within the structure of TDP-43, all of these processes will either be stopped, or will be influenced in a negative way (3). The TDP-43 is a complex and highly flexible protein mainly located in the cell nucleus and plays a vital role in DNA metabolism (3). Due to the high flexibility in the protein, it is very difficult to obtain the high-resolution structure of the full TDP-43 protein. However, machine learning tools like AlphaFold can be used to predict the complete 3D structure of the protein (4). The 3D structure of the protein is shown in Figure 1. Based on the structural studies, it contains three functional regions, i.e., (1) N-terminal domain; (2) DNA recognition motif (RRM1 and RRM2); and (3) Glycine-rich c-terminal domain. The N-terminal domain helps in directing TDP-43 protein towards the nucleus for RNA processing. In addition, it also plays a role in protein-protein interactions, post-translational modification, stabilizing the cell structure, and maintaining the cellular processing. The RNA recognition motifs (RRM1 and RRM2) responsible for the RNA recognition, its binding and processing (5). These proteins are the only rigid region of the protein and the 3D structure of these proteins can be obtained experimentally. Finally, the glycine-rich c-terminal domain contains multiple glycine in it and is responsible for the protein-protein interactions in the cell. TAR DNA-binding protein 43 (TDP-43) is coded by the TADRP gene and is a vital protein in the cell and is involved in several cellular processes including transport, RNA splicing, and transcription regulation (6). TDP-43 is composed of 414 amino acids and has two regions called DNA recognition motifs (RRMs) that enable

it to bind RNA and DNA. TDP-43 binds to UG-rich sequences in DNA, aiding the cell in regulating DNA splicing and gene expression. If it is mutated, neurodegenerative diseases are more likely to become a problem.

Molecular docking is a technique used to predict the orientation and the strength of a bond between one molecule(ligand) and another molecule(receptor) (7). This approach is usually used in drug discovery to study the interactions between potential drugs and different dangerous cells in a human body before clinical trials are conducted (7). Thousands of variations of one ligand are tested on one mutated cell or macromolecule, and the strength and interactions between the ligand and receptor are recorded to find the best suited ligand variation for a cer- tain drug (7). These ligands are then further evaluated based on numerous variables to test the practicality of the ligand and whether it can be used in a real-life setting (7).

Due to the highly disordered nature of the TDP-43 protein, a well structure of the protein is not available. Targeting TDP- 43 could be a key feature of several neurodegenerative diseases such as frontotemporal dementia (FTD) and amyotrophic lateral sclerosis (ALS). Since the RRM1 protein has a DNA-binding region, we hypothesize that inhibiting the mutated RRM1 protein by binding ligands to this region will also inhibit the TDP-43 protein, thereby reducing cell proliferation. Therefore, in the current research work we have performed molecular docking simulations using the AutoDock Vina software to predict the ligands that can inhibit the RRM1 protein of TDP-43. Inhibiting the TDP-43 protein will help in developing therapeutic strategies against various neurodegenerative diseases.

2. RESULTS

In this section we have discussed the molecular docking approach and the ligands obtained. TAR DNA-binding protein 43 (TDP-43) is a nuclear RNA/DNA binding protein that can shuttle between the nucleus and the cytoplasm. TDP-43 participates in splicing, transcriptional regulation, genomic stability in the nucleus, and DNA metabolism in the cytoplasm. The mutated TDP-43 accumulates in the mitochondria of neurons in various neurodegenerative diseases. Such as amyotrophic lateral sclerosis (ALS) and frontotemporal dementia (FTD). TDP-43 is a complex and flexible protein and obtaining a crystallized structure of this protein is very difficult. Therefore, only the rigid and more defined region has been obtained. RRM1 protein is involved in the synthesis of DNA and plays an important role in DNA binding and inhibiting this protein could potentially restrict the mutated TDP-43 protein functioning. Consequently, the RRM1 protein was utilized in this study, and small molecule inhibitors against this protein were found.

The electrostatic surface potential (ESP) of the protein is shown in Figure 2a. Based on the ESP the charge of the RRM1 protein is mostly positive; however, few negative regions were also observed in the protein. The positive charge might be associated with the negatively charged DNA. We hypothesize that the ligands/inhibitors should bind to a specific binding site of the RRM1 protein. To predict that this site is the druggable site we have utilized graph neural networks (GNN) using Graph Attention Site Prediction (GrASP) web server. Unlike traditional neural networks that handle structured data like images or sequences, GNNs can capture the relationships and interactions between nodes in a graph. The molecules are represented as graphs where atoms are nodes and bonds are edges. The attention mechanism then highlights the most critical parts of the graph and shows the potential drug binding site. The druggable site is shown in Figure 2b. Based on this the druggable site is shown in yellow and green in color which is the same as the EGF binding site. The druggable site represents the ability to effectively target and bind drugs to specific sites on proteins. Identifying druggable sites is crucial for designing therapeutics that can bind to these biomolecules.

In the next step molecular docking simulation of the RRM1 protein and ligands were performed using the AutoDock Vina software which gave five ligands that bind strongly to the protein. Based on our docking simulations, we have proposed five ligands (Ligand I, II, III, IV, and V) that bind strongly to the RRM1 protein. The interactions of these ligands with the RRM1 protein are shown in Figure 3 as a 2D representation. Ligand I and II formed both hydrophobic (in red eyelashes) and hydrogen bonds interactions. Ligand III showed less interactions, while Ligand IV and V formed mostly hydroponic interactions.

The spatial arrangement (3D) of these ligands on the protein is shown in Figure 4. Based on this only Ligand III, IV, and V bind to the druggable/DNA binding site of the protein. Ligands 1 and 2 had the most hydrophobic interactions and π-Cation interactions, while ligand 3 had the most hydrogen bonds. Ligand 3 had the least hydrophobic interactions, and ligand 4 had the least amount of hydrogen bonds and π-Cation interactions. Since ligand 3 had the most hydrogen bonds, it would be the most drug-like ligand out of the top 5. Ligand I and II did not bind to the druggable site. The RRM1-ligands chemical interactions were computed using PLIP web server, Table 1. Based on this, **Ligand I** formed six hydrophobic interactions with Thr116 (3.79Å), Glu117 (3.61Å), Val135 (3.64 and 3.66Å), Lys137 (3.39Å), and His143 (3.89Å). In addition, it forms one hydrogen bond with Ser144 (2.44Å), and two π-Cation Interactions with Lys137 (4.28Å) and His143 (4.38Å). **Ligand II** formed 6 hydrophobic interactions with Thr116(3.77Å), Glu117(3.65Å), Val135(3.66 and 3.69Å), and His143(1.28Å). Additionally, Ligand II also formed one hydrogen bond with Ser144(2.44Å), and 2 π-Cation interactions with Lys137(4.30Å) and His143(1.28Å). **Ligand III** interacts with Thr115(3.76Å), Asp119(3.55Å), and Ile168(3.78Å) to form 3 hydrophobic interactions. Ligand III also forms 6 hydrogen bonds with Lys114(3.53 and 3.22Å), Asp119(3.61 and 3.13Å), Glu122(2.98Å), and Gly169(2.42Å), and one π-Cation interaction with TYR123(4.78Å). **Ligand IV** forms 4 hydrophobic interactions with Thr115(4.00Å), Glu122(3.91Å), Tyr123(3.72Å), and Ile168(3.55Å). **Ligand V** forms 4 hydrophobic interactions with Thr115(3.66Å), Asp119(3.58Å), Tyr123(3.76Å), and Ile168(3.89Å). Ligand V also forms 4 hydrogen bonds with Glu122(3.60 and 3.14Å), Met167(2.69Å), and Ile168(3.89Å) and one π-Cation interaction with Tyr123(4.84Å).

To assess each ligand's pharmacological characteris- tics, we used the SwissADME online server to simulate the lig- ands' absorption, distribution, metabolism, and excretion (Ta- ble 2).Several techniques are employed to assess the ligands, including the Lipinsky rule, blood brain barrier (BBB) penetration, and gastrointestinal (GI) absorption. GI absorption measures the permeability and transit rate of the drug through the GI tract. To measure if the drug will pass through the semipermeable membrane between the blood and the brain, the BBB permeation test is utilized. To measure how likely a compound will be to be a viable active drug for humans. Based on the results, all the ligands have high GI absorption, and most show BBB permeation (table 2), with only ligand I not showing permeation. Furthermore, all ligands passed the Lipinsky rule, suggesting that the ligands show high drug likeliness.

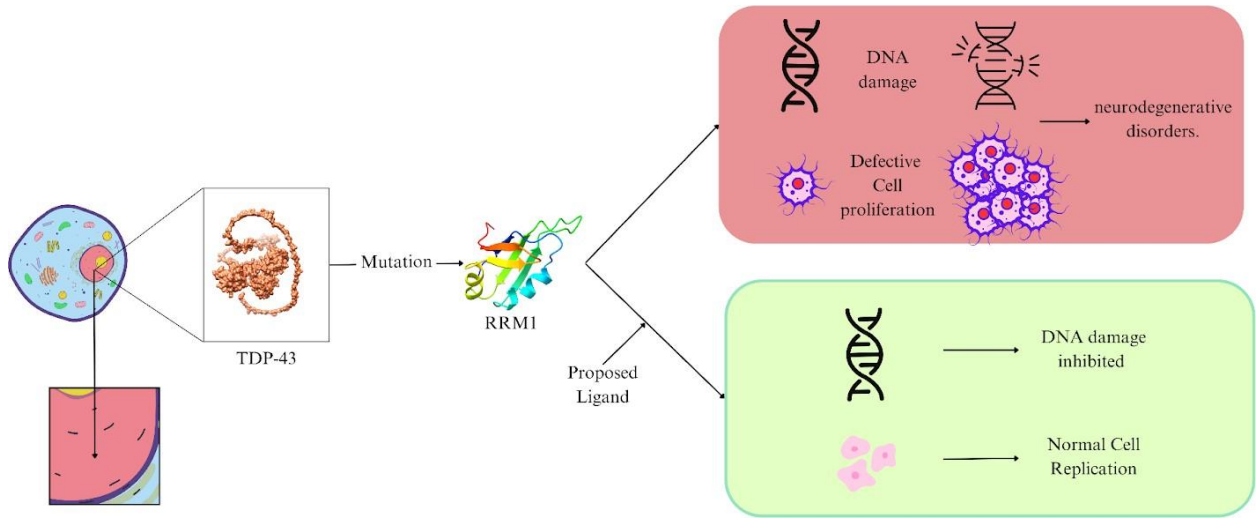

Fig. 1. Dysregulation of TDP-43 protein. The figure shows that the TDP-43 is a flexible and complex protein is present in the nucleus. Mutation in the RRM1 protein (rigid segment of TDP-43) results in the DNA damage and defective cell proliferation (shown in red box). In the current research work we have proposed RRM1 targeted ligands that could mitigative this problem (shown in green box).

3. DISCUSSION

Based on experiential studies RRM1 protein is the DNA binding region of the TDP-43 protein hence, we have targeted this protein for our studies (8). A minimum of two and a maximum of eight nucleotides can interact with each RRM, either generically or sequence-specifically. RNA-recognition motif (RRM) RRM-containing proteins participate in various post-transcriptional RNA processing, such as mRNA splicing, editing, export, stability regulation and turnover. All of the RRM structures reported to date show that RRM binds single-stranded RNA or DNA.

The electrostatic surface potential (ESP) of the protein is shown in Figure 6b. Based on the ESP, the active site and its vicinity are positive in nature (shown in blue color). This could be the driving force to attract the negative charged DNA. To further evaluate the TDP-43 protein DNA binding mechanism, we have also used the newly released AlphaFold 3 machine learning tool. The tool predicts the structure and interactions of proteins, DNA, RNA, and ligands. The AlphaFold 3 predicted structure, the DNA binds only to the RRM1 of the protein (9). The DNA interacts with the positively charged DNA binding site of the protein. This structure could be accurate because the negatively charged DNA binds only to the positive region of the protein. This also shows that significant conformational changes are required for DNA binding and processing. Based on previous studies, the RRM1 has a high affinity for DNA and plays an important role in the initial DNA binding. To find the conformational changes that happen in the protein, a normal mode analysis (NMA) was also performed, which is used to describe the possible flexible states of the protein. Based on NMA, the three domains of the protein breathe and make a rock and roll motion, as shown in Figure 5. A similar breathing mechanism has also been observed in other proteins like GpdQ (10).

Molecular docking simulations, while powerful, have several limitations that impact their accuracy and reliability (11). One primary limitation is the simplification of the molecular interactions involved (11). These simulations often rely on approximations and assumptions to model complex biological environments, which can lead to inaccuracies in predicting binding affinities and conformations. Additionally, the quality of the input structures significantly affects the results; any errors in the protein or ligand structures can propagate through the simulation, leading to misleading outcomes. The scoring functions used to evaluate docking pose also present challenges, as they may not adequately capture the nuances of molecu- lar interactions, such as entropic effects and solvent dynamics. Furthermore, computational docking simulations can be computationally expensive and time-consuming, especially when dealing with large systems or when high accuracy is required. Finally, despite algorithms and computational power advances, these simulations still cannot fully replicate the dynamic nature of biological systems, limiting their predictive power and applicability in drug discovery and other fields.

In conclusion, we have used molecular docking simulations to identify potential inhibitors targeting the RRM1 region of the TDP-43, a protein linked to neurodegenerative diseases like ALS and FTD. Based on docking results, five ligands were selected that bind strongly to the RNA binding region of the protein and could potentially inhibit the TDP-43 functioning. the docking

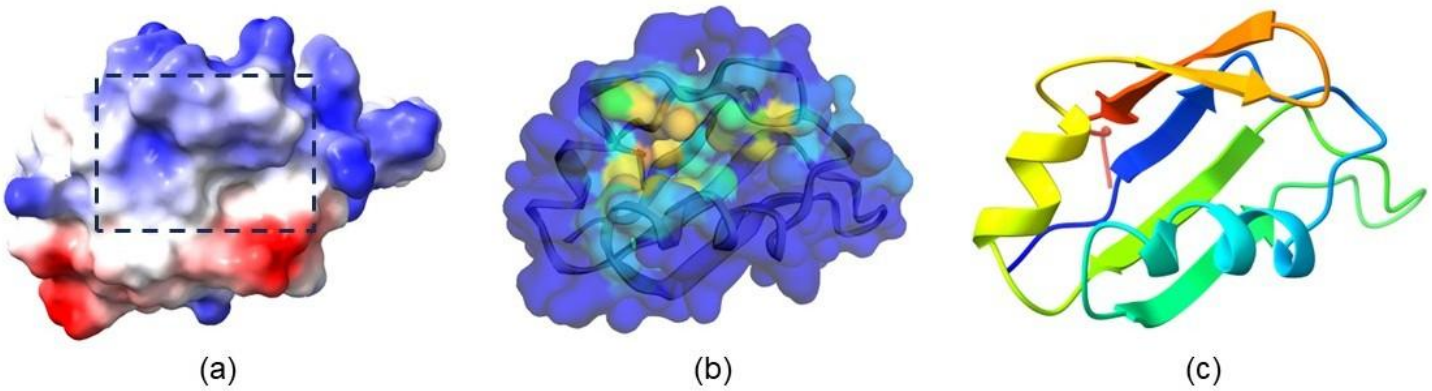

Fig. 2. The electrostatic surface potential (ESP) and druggable site. (a) based on the ESP of the RRM1 protein the DNA binding site is positively charged and hence attracts DNA; (b) druggable site and DNA binding site are same. Our docked ligands also bind to this region; and (c) the RRM1 protein structure is shown for comparison.

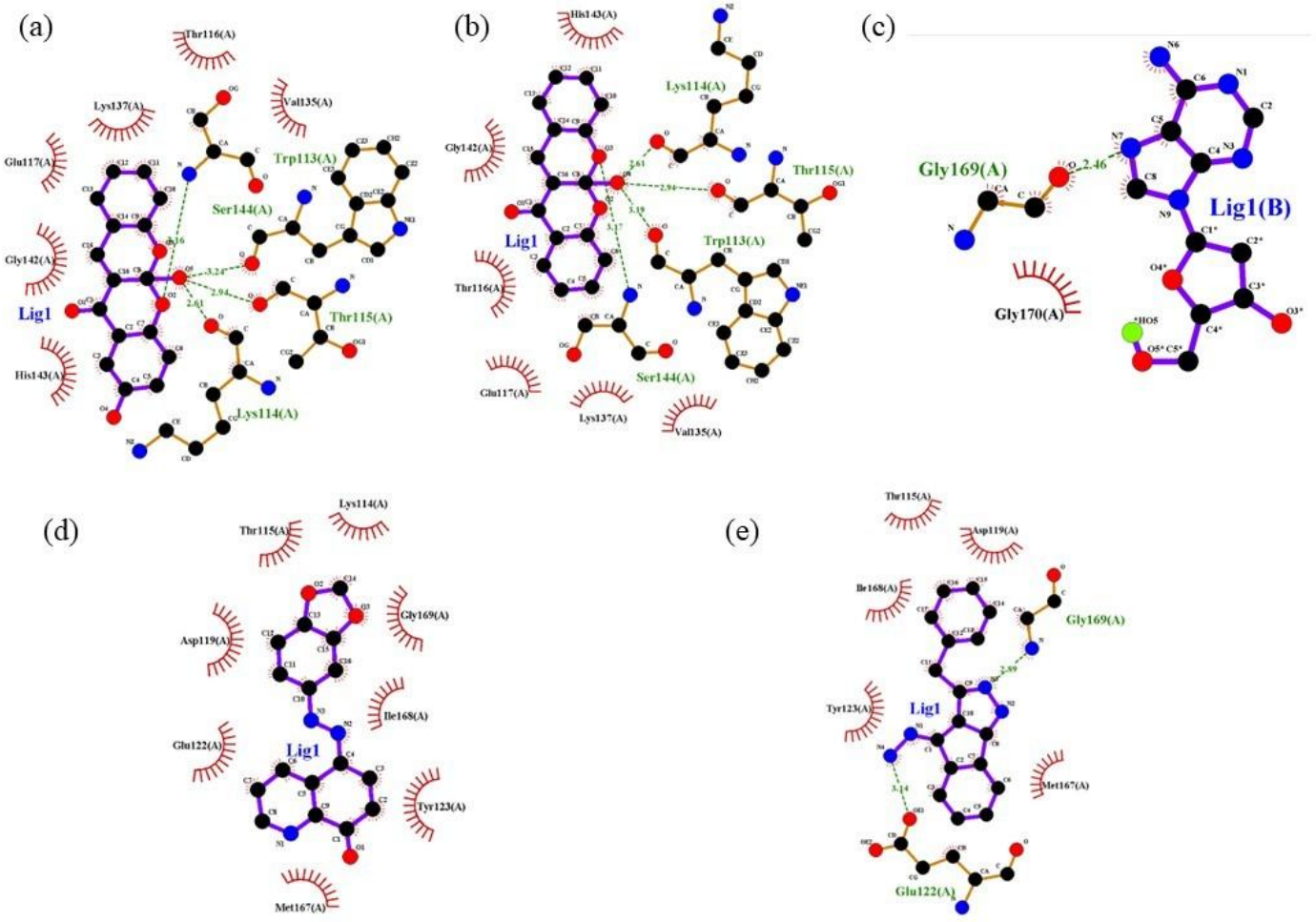

Fig. 3. 2D protein-ligand interactions. Based on this image (a) and (b) both hydrophobic and hydrogen bonds were observed; (c) few interactions were observed; in (d) and (e) mostly hydrophobic interactions were observed. Hydrophobic bonds are in red eyelashes and hydrogen bonds in green lines.

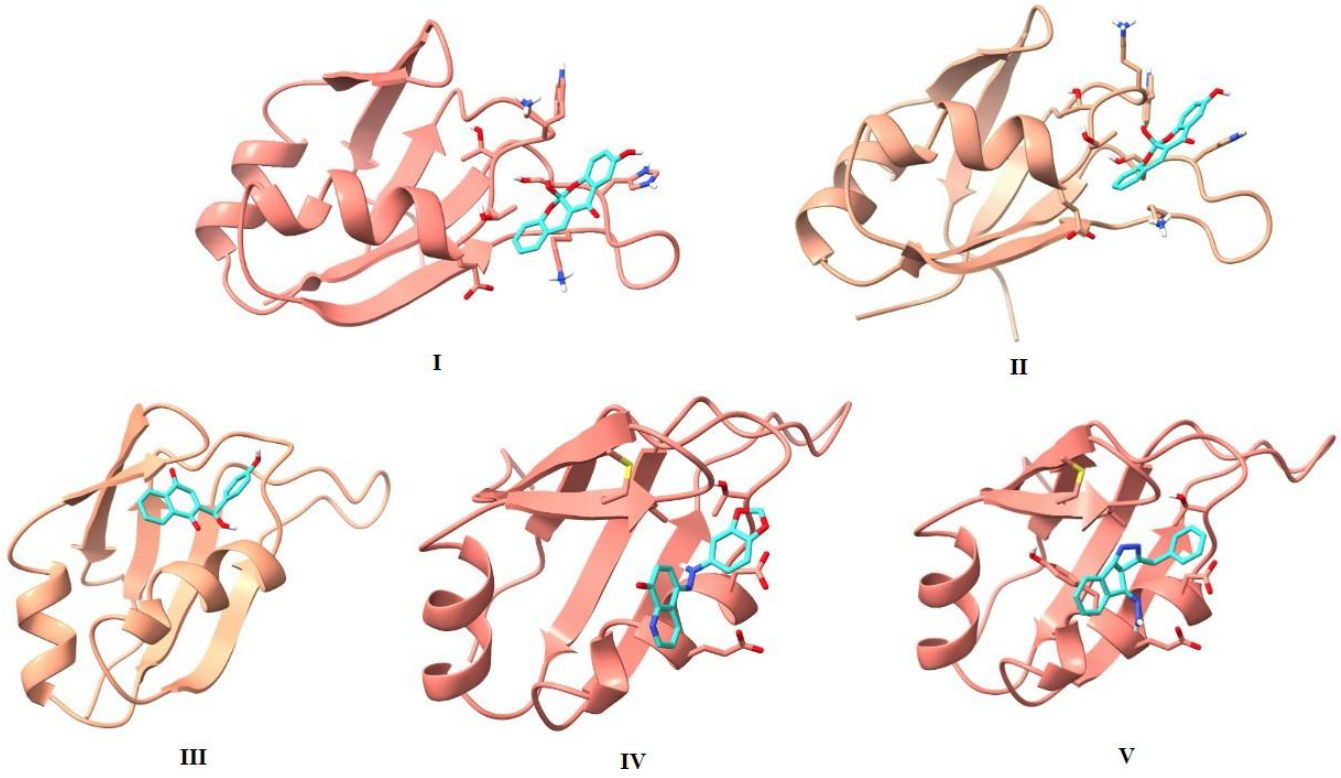

Fig. 4. Protein-ligand interactions. 3D structure of RRM1-ligand interactions. The RRM1 protein is in pink and ligands are in cyan. All the ligands bind to the DNA binding region of the protein.

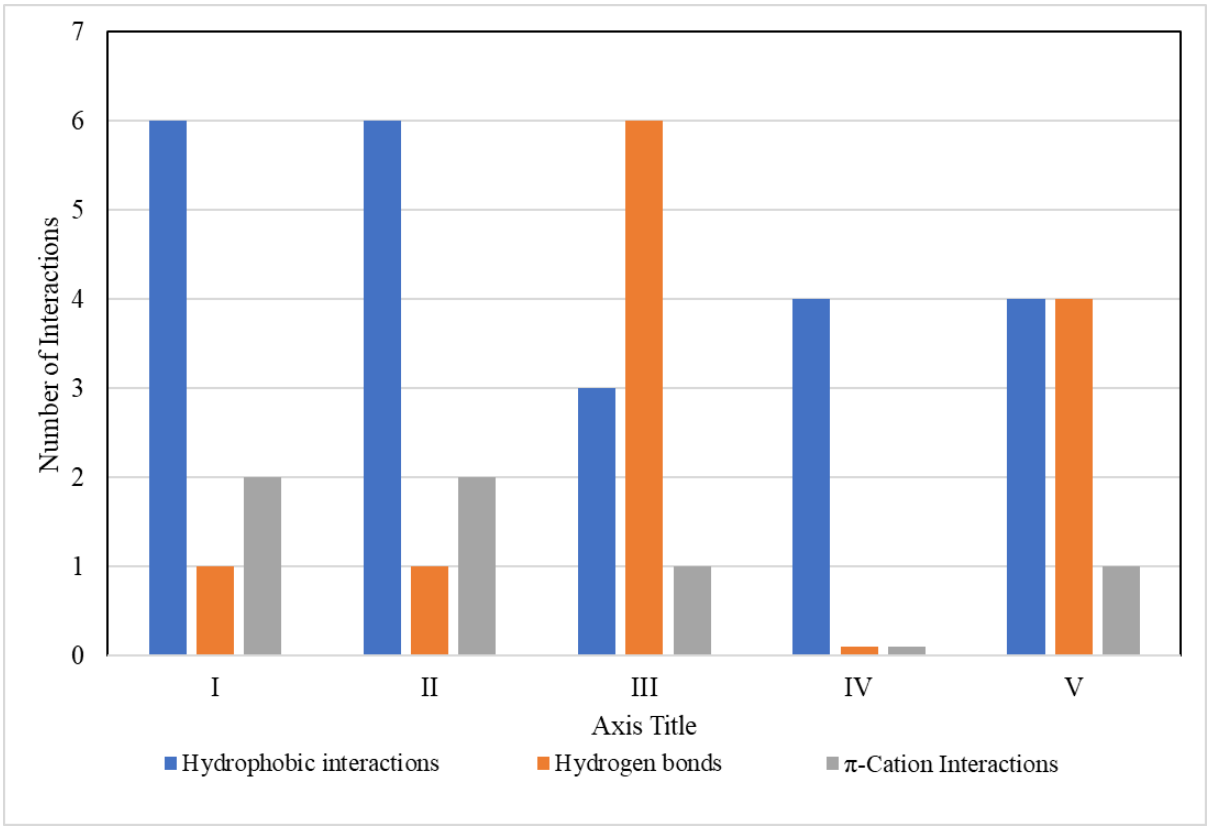

Fig. 5. RRM1-ligand interactions. The graph shows that all three types of interactions hydrogen bonds, hydrophobic interactions and π cation interactions were observed in the protein-ligands interactions.

Table 1. Protein-ligand interactions. The hydrophobic and hydrogen bond interactions formed between the amino acids and nucleotides are the driving force between their interactions. The distances are shown in the Angstrom (Å) unit.

I		
Types of interactions	**Amino acid**	**Distance (Å)**
	Thr116	3.79
	Glu117	3.61
Hydrophobic interactions	Val135	3.64, 3.66
	Lys137	3.39
	His143	3.89
Hydrogen bonds	Ser144	2.44
	Lys137	4.28
***π*-Cation interactions**	His143	4.38
II		
	Thr116	3.77
	Glu117	3.65
Hydrophobic interactions	Val135	3.66, 3.69
	Lys137	3.35
	His143	3.91
Hydrogen bonds	Ser144	2.44
	Lys137	4.30
***π*-Cation interactions**	His143	1.28
III		
	Thr115	3.76
Hydrophobic interactions	Asp119	3.55
	Ile168	3.78
Hydrogen bonds	Lys114	3.53, 3.22
	Asp119	3.61, 3.13
	Glu122	2.98
	Gly169	2.42
***π*-Cation interactions**	Tyr123	4.78
IV		
Hydrophobic interactions	Thr115	4.00
	Glu122	3.91
	Tyr123	3.72
	Ile168	3.55
V		
	Thr115	3.66
Hydrophobic interactions	**Asp119**	**3.58**
	Tyr123	**3.76**
	Ile168	**3.89**
	Glu122	3.60, 3.14
Hydrogen bonds	**Met167**	**2.69**
	Gly169	**2.42**
***π*-Cation interactions**	Tyr123	4.84

Table 2. The pharmaceutical properties of the five ligands were computed using the SwissADME web server. GI absorption indicates that the drug passes through the gastrointestinal tract into the bloodstream. BBP permeation refers to the ability of a drug to cross the blood-brain barrier and reach the central nervous system. Drug likeliness (Lipinski's Rule of Five) consists of a set of criteria predicting a compound's drug likeliness.

	I	**II**	**III**	**IV**	**V**
Formula, molecular weight	282.25	266.25	280.27	293.28	274.32
GI absorption	High	High	High	High	High
BBB permeation	No	Yes	Yes	Yes	Yes
Drug likeliness (Lipinski)	Yes	Yes	Yes	Yes	Yes
2D structure					

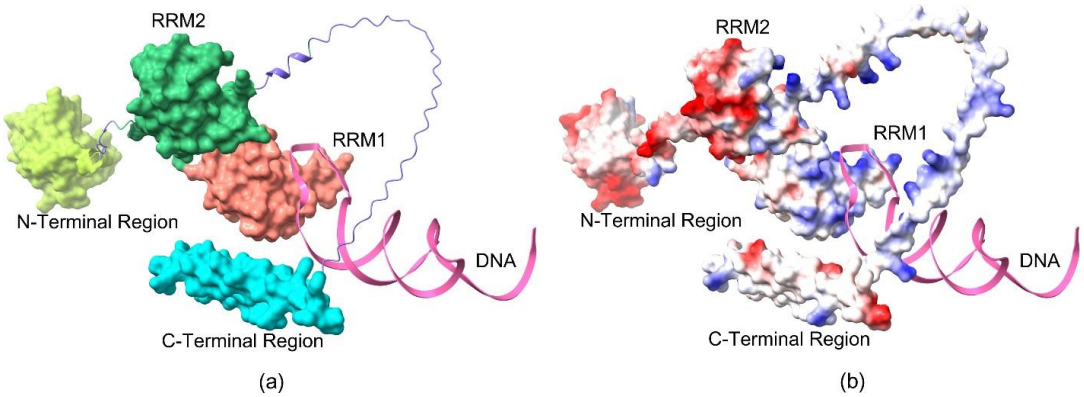

Fig. 6. Proposed 3D structure of DNA bound TDP-43 protein. (a) The TDP-43 protein has four defined regions N-terminal re- gion, RRM1, RRM2, and C-terminal region. Our predicted structure shows that the DNA binds to the RRM1 protein. Based on our knowledge this is the first time complete TDP-43-DNA complex structure is predicted. Experimental studies have also showed that the RRM1 protein is the DNA binding region; and (b) The electrostatic surface potential (ESP) of the protein shows that N- terminal and RRM2 domains are mostly negative (in red), C-Terminal region is neutral (while) and RRM1 is mostly positive (blue). This also explains the binding of highly negative DNA to the RRM1 protein.

results were further validated using the electrostatic surface potential ESP and predicting the druggable site of the protein. Later the pharmacological properties of the selected ligands shows that the ligands have high GI absorption and BBB permeation (except Ligand I). Finally, the 3D structure of TDP-43 bound with RNA has also been elucidated and based on our knowledge this is the first time the 3D structure of TDP-43 bound with RNA has been obtained. The work will help in understanding the functioning and mechanism of TDP-43 in RNA processing and will aid in developing a foundational framework for drug development process against neurodegenerative.

4. METHOD

The three-dimensional structure of the RRM1 region of TDP-43 was obtained from the Protein Data Bank (PDB ID: 4y00) (1). Ligands were obtained from the Zinc20 Database, and roughly 5000 compounds were selected for virtual screening (12). The following are the Zinc Database Tranches settings that were used when downloading ligand files: (1) only 3D models were selected; (2) in the reactivity section, "Standard" and "Exclusive" were chosen; (3) in purchasability, "In-Stock" and "Exclusive" options were selected; (4) Reference (R) pH was chosen; (5) Charge: "0"; and (6) "Lead-Like" compounds were selected. ligands were selected based on their LogP values. Since chemical compounds with a LogP value of 2 have good oral and intestinal absorption, only these compounds were selected for virtual screening. All of the compounds were downloaded in PDBQT file format. The binding poses of ligands to the ZnT opening were found and examined using AutoDock Vina 1.5.6 software (13). 10 poses were generated for all four protein-substrate complexes for each protocol. The Autodock scoring method was used to select the top five candidates that showed strong binding with the RRM1 region. The scoring criteria is based on if the ligand fits in the binding site, if it forms strong interactions with the protein, and how strong these bonds are. Protein Ligand Interaction Profiler (PLIP) web server was utilized to obtain the protein-ligand interactions (14). To visualize and evaluate the protein-ligand complexes, the ChimeraX and PyMol were used (15,16). SwissADME was used to assess the pharmacological and carcinogenic properties of the compounds (17). The 3D structure of singular RNA bound TDP-43 protein was obtained using AlphaFold 3 (4).

Protein-ligand interactions. The hydrophobic and hydrogen bond interactions formed between the amino acids and nucleotides are the driving force between their interactions. The distances are shown in the Angstrom (Å) unit.

The pharmaceutical properties of the five ligands were computed using theSwissADME web server. GI absorption indicates that the drug passes through the gastrointestinal tract into the bloodstream. BBP permeation refers to the ability of a drug to cross the blood-brain barrier and reach the central nervous system. Drug likeliness (Lipinski's Rule of Five) consists of a set of criteria predicting a compound's drug likeliness.

5. REFERENCES

1. Chiang, C.H. et al. "Structural analysis of disease-related tdp-43 d169g mutation: Linking enhanced stability and caspase cleavage efficiency to protein accumulation." Scientific reports, vol. 6, 2016, p. 21581. https://doi.org/10.1038/srep21581.
2. Tetter, S. et al. "Taf15 amyloid filaments in frontotemporal lobar degeneration." Nature, vol. 625, no. 7994, 2024, pp. 345-351. https://doi.org/10.1038/s41586-023-06801-2.
3. Buratti, E. "Functional significance of tdp-43 mutations in disease." Advances in genetics, vol. 91, no. 1, 2015, pp. 1-53. https://doi.org/10.1016/bs.adgen.2015.07.001
4. Abramson, J. et al. "Accurate structure prediction of biomolecular interactions with alphafold 3." Nature, vol. 630, no. 8016, 2024, pp. 493-500. https://doi.org/10.1038/s41586-024-07487-w.
5. Cléry, A. et al. "Rna recognition motifs: Boring? Not quite." Current Opinion in Structural Biology, vol. 18, no. 3, 2008, pp. 290-298. https://doi.org/10.1016/j.sbi.2008.04.002.
6. Paulson, H.L. et al. "Genetics of dementia." Semin Neurol, vol. 31, no. 05, 2011, pp. 449-460. https://doi.org/10.1055/s-0031-1299784.
7. Fan, J. et al. "Progress in molecular docking." Quantitative Biology, vol. 7, no. 2, 2019, pp. 83-89. https://doi.org/10.1007/s40484-019-0172-y.

8. Jiang, Y.X. et al. "Amyloid fibrils in ftld-tdp are composed of tmem106b and not tdp-43." Nature, vol. 605, no. 7909, 2022, pp. 304-309. https://doi.org/10.1038/s41586-022-04670-9.
9. Goedert, M. "Alpha-synuclein and neurodegenerative diseases." Nature Reviews Neuroscience, vol. 2, no. 7, 2001, pp. 492-501. https://doi.org/10.1038/35081564.
10. Sharma, G. et al. "Investigating coordination flexibility of glycerophosphodiesterase (gpdq) through interactions with mono-, di-, and triphosphoester (npp, bnpp, gpe, and paraoxon) substrates." Physical Chemistry Chemical Physics, vol. 21, no. 10, 2019, pp. 5499-5509. https://doi.org/10.1039/C8CP07031H.
11. Korb, O. et al. "Potential and limitations of ensemble docking." Journal of Chemical Information and Modeling, vol. 52, no. 5, 2012, pp. 1262-1274. https://doi.org/10.1021/ci2005934.
12. Irwin, J.J. et al. "Zinc20—a free ultralarge-scale chemical database for ligand discovery." Journal of Chemical Information and Modeling, vol. 60, no. 12, 2020, pp. 6065-6073. https://doi.org/10.1021/acs.jcim.0c00675.
13. Trott, O. et al. "Autodock vina: Improving the speed and accuracy of docking with a new scoring function, efficient optimization, and multithreading." Journal of computational chemistry, vol. 31, no. 2, 2010, pp. 455-461. https://doi.org/10.1002/jcc.21334
14. Salentin, S. et al. "Plip: Fully automated protein–ligand interaction profiler." Nucleic Acids Research, vol. 43, no. W1, 2015, pp. W443-W447. https://doi.org/10.1093/nar/gkv315.
15. Pettersen, E.F. et al. "Ucsf chimerax: Structure visualization for researchers, educators, and developers." Protein science, vol. 30, no. 1, 2021, pp. 70-82. https://doi.org/10.1002/pro.3943.
16. Yuan, S. et al. "Using pymol as a platform for computational drug design." Wiley Interdisciplinary Reviews: Computational Molecular Science, vol. 7, no. 2, 2017, p. e1298. https://doi.org/10.1002/wcms.1298
17. Schwede, T. et al. "Swiss-model: An automated protein homology-modeling server." vol. 31, no. 13, 2003, pp. 3381-3385. https://doi.org/10.1093/nar/gkg520

Table 1. Protein-ligand interactions. The hydrophobic and hydrogen bond interactions formed between amino acids and nucleotides are the driving forces behind their interactions. The distances are expressed in Angstroms (Å).

I		
Types of interactions	**Amino acid**	**Distance (Å)**
	Thr116	3.79
	Glu117	3.61
Hydrophobic interactions	Val135	3.64, 3.66
	Lys137	3.39
	His143	3.89
Hydrogen bonds	Ser144	2.44
	Lys137	4.28
π-Cation interactions	His143	4.38
II		
	Thr116	3.77
	Glu117	3.65
Hydrophobic interactions	Val135	3.66, 3.69
	Lys137	3.35
	His143	3.91
Hydrogen bonds	Ser144	2.44
	Lys137	4.30
π-Cation interactions	His143	1.28
III		
	Thr115	3.76
Hydrophobic interactions	Asp119	3.55
	Ile168	3.78
Hydrogen bonds	Lys114	3.53, 3.22
	Asp119	3.61, 3.13
	Glu122	2.98
	Gly169	2.42
π-Cation interactions	Tyr123	4.78
IV		
Hydrophobic interactions	Thr115	4.00
	Glu122	3.91
	Tyr123	3.72
	Ile168	3.55
V		
	Thr115	3.66
Hydrophobic interactions	**Asp119**	**3.58**
	Tyr123	**3.76**
	Ile168	**3.89**
	Glu122	3.60, 3.14
Hydrogen bonds	**Met167**	**2.69**
	Gly169	**2.42**
π-Cation interactions	Tyr123	4.84

Table 2. The pharmaceutical properties of the five ligands were computed using the SwissADME web server. GI absorption indicates that the drug passes through the gastrointestinal tract into the bloodstream. BBP permeation refers to the ability of a drug to cross the blood-brain barrier and reach the central nervous system. Drug likeliness (Lipinski's Rule of Five) consists of a set of criteria predicting a compound's drug likeliness.

	I	**II**	**III**	**IV**	**V**
Formula, molecular weight	282.25	266.25	280.27	293.28	274.32
GI absorption	High	High	High	High	High
BBB permeation	No	Yes	Yes	Yes	Yes
Drug likeliness (Lipinski)	Yes	Yes	Yes	Yes	Yes
2D structure					